Multimodal prediction of residual consciousness in the intensive care unit: the CONNECT-ME study

Moshgan Amiri, Patrick M Fisher, Federico Raimondo, Annette Sidaros, Melita Cacic Hribljan, Marwan H Othman, Ivan Zibrandtsen, Simon S Albrechtsen, Ove Bergdal, Adam Espe Hansen, et al.

BRAIN
ORIGINAL ARTICLE

Multimodal prediction of residual consciousness in the intensive care unit: the CONNECT-ME study

Moshgan Amiri,[1,†] Patrick M. Fisher,[2,†] Federico Raimondo,[3,4,†] Annette Sidaros,[1,5] Melita Cacic Hribljan,[5] Marwan H. Othman,[1] Ivan Zibrandtsen,[5] Simon S. Albrechtsen,[1] Ove Bergdal,[6] Adam Espe Hansen,[7,8] Christian Hassager,[8,9] Joan Lilja S. Højgaard,[1] Elisabeth Waldemar Jakobsen,[1] Helene Ravnholt Jensen,[10] Jacob Møller,[9] Vardan Nersesjan,[1,11] Miki Nikolic,[5] Markus Harboe Olsen,[10] Sigurdur Thor Sigurdsson,[10] Jacobo D. Sitt,[12] Christine Sølling,[10] Karen Lise Welling,[10] Lisette M. Willumsen,[6] John Hauerberg,[6] Vibeke Andrée Larsen,[7] Martin Fabricius,[5,8] Gitte Moos Knudsen,[2,8] Jesper Kjaergaard,[8,9] Kirsten Møller[8,10] and Daniel Kondziella[1,8]

[†]These authors contributed equally to this work.

See Claassen (https://doi.org/10.1093/brain/awac434) for a scientific commentary on this article.

Functional MRI (fMRI) and EEG may reveal residual consciousness in patients with disorders of consciousness (DoC), as reflected by a rapidly expanding literature on chronic DoC. However, acute DoC is rarely investigated, although identifying residual consciousness is key to clinical decision-making in the intensive care unit (ICU). Therefore, the objective of the prospective, observational, tertiary centre cohort, diagnostic phase IIb study 'Consciousness in neurocritical care cohort study using EEG and fMRI' (CONNECT-ME, NCT02644265) was to assess the accuracy of fMRI and EEG to identify residual consciousness in acute DoC in the ICU. Between April 2016 and November 2020, 87 acute DoC patients with traumatic or non-traumatic brain injury were examined with repeated clinical assessments, fMRI and EEG. Resting-state EEG and EEG with external stimulations were evaluated by visual analysis, spectral band analysis and a Support Vector Machine (SVM) consciousness classifier. In addition, within- and between-network resting-state connectivity for canonical resting-state fMRI networks was assessed. Next, we used EEG and fMRI data at study enrolment in two different machine-learning algorithms (Random Forest and SVM with a linear kernel) to distinguish patients in a minimally conscious state or better (≥MCS) from those in coma or unresponsive wakefulness state (≤UWS) at time of study enrolment and at ICU discharge (or before death). Prediction performances were assessed with area under the curve (AUC). Of 87 DoC patients (mean age, 50.0 ± 18 years, 43% female), 51 (59%) were ≤UWS and 36 (41%) were ≥MCS at study enrolment. Thirty-one (36%) patients died in the ICU, including 28 who had life-sustaining therapy withdrawn. EEG and fMRI predicted consciousness levels at study enrolment and ICU discharge, with maximum AUCs of 0.79 (95% CI 0.77–0.80) and 0.71 (95% CI 0.77–0.80), respectively. Models based on combined EEG and fMRI features predicted consciousness levels at study enrolment and ICU discharge with maximum AUCs of 0.78 (95% CI 0.71–0.86) and 0.83 (95% CI 0.75–0.89), respectively, with improved positive predictive value and sensitivity. Overall, both machine-learning algorithms (SVM and Random Forest) performed equally well. In conclusion, we suggest that acute DoC prediction models in the ICU be based on a combination of fMRI and EEG features, regardless of the machine-learning algorithm used.

Received April 27, 2022. Revised July 25, 2022. Accepted August 14, 2022. Advance access publication September 13, 2022

1 Department of Neurology, Copenhagen University Hospital, Rigshospitalet, Copenhagen, Denmark
2 Neurobiology Research Unit, Copenhagen University Hospital, Rigshospitalet, Copenhagen, Denmark
3 Institute of Neuroscience and Medicine, Brain and Behaviour (INM-7), Research Center Jülich, Jülich, Germany
4 Institute of Systems Neuroscience, Medical Faculty, Heinrich Heine University Düsseldorf, Düsseldorf, Germany
5 Department of Neurophysiology, Copenhagen University Hospital, Rigshospitalet, Copenhagen, Denmark
6 Department of Neurosurgery, Copenhagen University Hospital, Rigshospitalet, Copenhagen, Denmark
7 Department of Radiology, Copenhagen University Hospital, Rigshospitalet, Copenhagen, Denmark
8 Department of Clinical Medicine, University of Copenhagen, Copenhagen, Denmark
9 Department of Cardiology, Copenhagen University Hospital, Rigshospitalet, Copenhagen, Denmark
10 Department of Neuroanaesthesiology, Copenhagen University Hospital, Rigshospitalet, Copenhagen, Denmark
11 Biological and Precision Psychiatry, Copenhagen Research Center for Mental Health, Copenhagen University Hospital, Copenhagen, Denmark
12 Sorbonne Université, Institut du Cerveau - Paris Brain Institute - ICM, Inserm, CNRS, APHP, Hôpital de la Pitié Salpêtrière, Paris, France

Correspondence to: Daniel Kondziella, MD, MSc, PhD
FEBN Department of Neurology
Copenhagen University Hospital, Rigshospitalet
Blegdamsvej 9, DK-2100 Copenhagen
E-mail: daniel.kondziella@regionh.dk

Keywords: acute brain injury; disorders of consciousness; EEG; functional MRI; machine-learning

Introduction

Acute brain injury is a medical and socioeconomic emergency. Traumatic brain injury alone results in 1.5 million hospital admissions and 57 000 deaths in the EU annually.[1] Of all comatose patients with TBI, 40% die in the intensive care unit (ICU) and 20% enter a prolonged disorder of consciousness (DoC), seemingly unaware of themselves and their environment.[2]

In clinical routine, the rate of patients with undetected consciousness is high. Healthcare professionals fail to identify residual consciousness in up to 40% of unresponsive patients with brain injury[3] and are challenged by unusual coma presentations.[4] As 70% of deaths in the ICU occur after withdrawal of life-sustaining therapy (WLST),[5] accurate assessment of consciousness levels is crucial to avoid flawed medical decision-making, including premature WLST owing to underestimation of residual consciousness.[6] Conversely, overestimation of consciousness levels after acute brain injury may lead to futile treatment, putting a strain on limited healthcare resources. This raises the important question: of all DoC patients with acute brain injury in the ICU, who has residual consciousness or the potential to recover it and who does not?

Complementing the clinical neurological examination, functional neuroimaging and EEG provide a means of assessing evidence for residual consciousness that does not require active motor responses from the patient.[7] Although highly specific in identifying covertly conscious patients, active mental task-based functional MRI (fMRI)[8] and EEG[9] paradigms often underestimate residual consciousness in DoC patients because of insufficient arousal and lack of sustained attention.[7,10] The typically fluctuating course of awareness in DoC patients, especially in the acute phase, is another obstacle.[11] Only 14% of unresponsive wakefulness syndrome (UWS) and 26% of minimally conscious state (MCS) patients can participate in active EEG/fMRI paradigms.[7] In contrast, passive paradigms (i.e. including external stimuli, but without request for command following) and resting-state EEG and fMRI do not require active effort on the part of the patient and might therefore be advantageous for assessment of residual consciousness in patients in the ICU.[12–14] Although American[15] and European[16] guidelines recommend EEG- and fMRI-based paradigms for the evaluations of consciousness levels, comparative studies of fMRI and EEG in large acute DoC cohorts in the ICU are lacking.[13,17,18]

Here, our objective was to measure the accuracy of fMRI and EEG to identify residual consciousness in acute DoC, in a prospective, observational, tertiary centre, ICU cohort, diagnostic phase IIb study. We analysed EEG data by three different methods and estimated resting-state fMRI between- and within-network connectivity. Next, we used EEG and fMRI features to predict consciousness level in acute DoC patients at two time points: time of clinical examination closest to EEG and fMRI recordings (study enrolment) and time of discharge from the ICU or death (ICU discharge), using two different machine-learning algorithms.

We hypothesized that multimodal assessment of residual consciousness by fMRI and EEG would effectively predict clinical diagnosis of consciousness in acute DoC patients in the ICU, and that by combining fMRI and EEG features even more accurate prognostication would be achieved.

Materials and methods

Figure 1 shows the study design, patient flow and data analysis strategy. A detailed study protocol has been published.[19]

Patients

Between April 2016 and November 2020, we included patients admitted to the ICUs at a tertiary referral centre (Rigshospitalet, Copenhagen University Hospital). Patients were included first on convenience basis (April 2016–August 2019, $n = 63$), then by systematic daily screening (September 2019–November 2020, $n = 25$) of the four ICUs at Rigshospitalet. All patients were enrolled prospectively during the ICU admission.

Inclusion criteria were: (i) DoC patients (age > 16 years) subclassified into coma, UWS, MCS−/MCS+,[20] emerged from MCS (eMCS),[21] confusional state (CS) or locked-in syndrome (LIS) (Supplementary

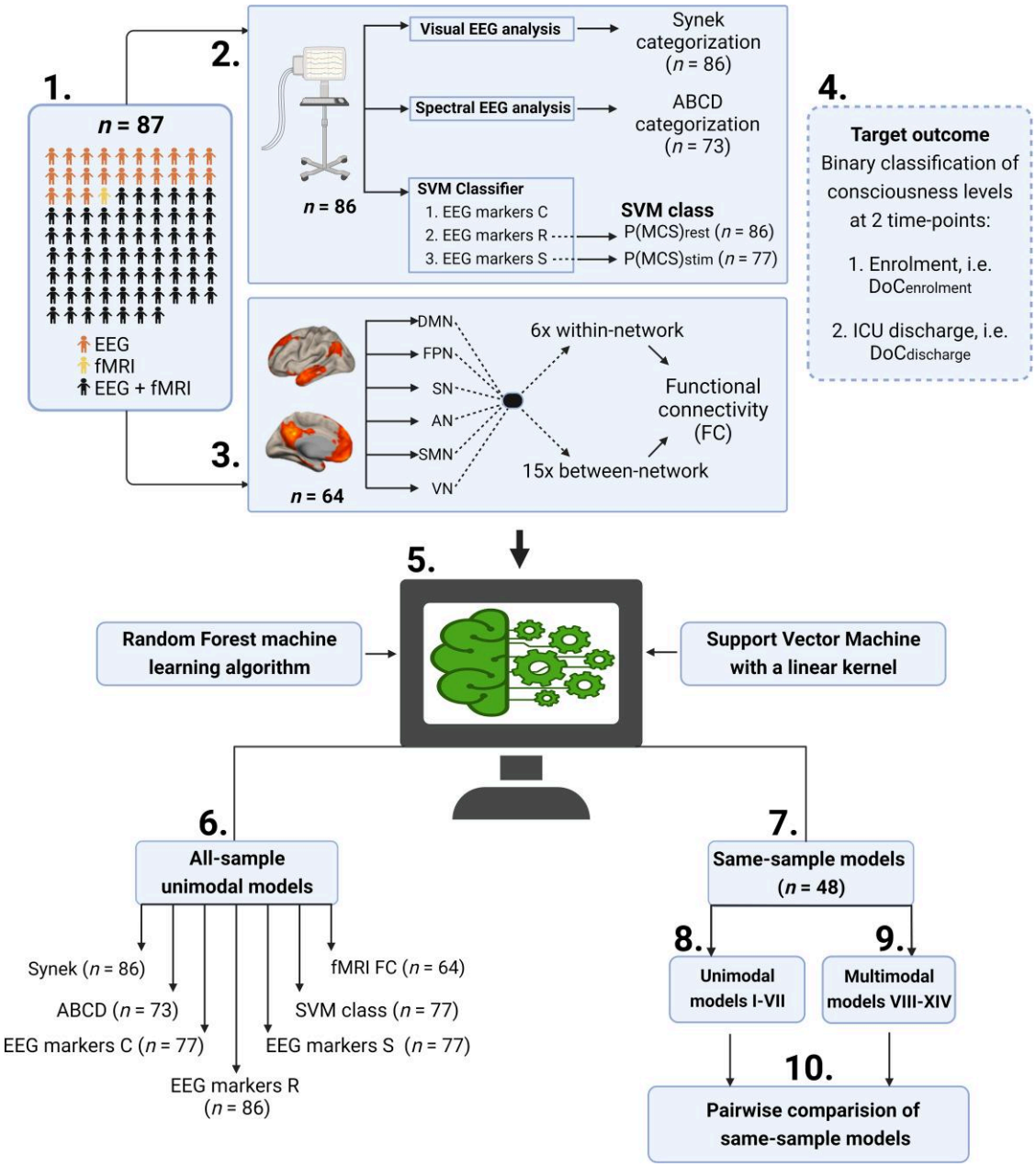

Figure 1 Flow chart and methods. (1) The study population consisted of 87 patients who were clinically classified according to their level of consciousness after ICU admission at study enrolment and ICU discharge (or prior to death). EEG was performed in 86 patients, fMRI in 64 patients and both EEG and fMRI in 63 patients (orange); in one patient (yellow) only fMRI was available and in 23 patients (dark grey) only EEG. (2) All EEGs were analysed using three different methods: manual visual analysis with grading according to the Synek scale; categorization according to the ABCD model based on spectral band power from centrally located EEG electrodes; automated classification using a SVM classifier based on 68 EEG markers from the whole EEG recording (EEG markers C), EEG markers R from resting-state EEG and EEG markers S from EEG with stimulations. (3) FMRI functional connectivity (FC) estimates were derived from six networks, resulting in six within-network and 15 between-network connectivity estimates. (4) Target outcomes to be predicted were consciousness levels at time of enrolment ($DoC_{enrolment}$) and at time of ICU discharge ($DoC_{discharge}$). (5) Prediction performance of all EEG and fMRI features were analysed using two different machine-learning algorithms: Random Forest and Support Vector Machine (SVM). (6) First, prediction performance of each available feature with maximum available data was determined with unimodal models (results are presented in Table 2). (7) Then, for direct comparison of models, same-sample models based on data from 48 patients with all available features (i.e. all six EEG features *and* fMRI FC measures) were derived (results are given in Table 3). (8) Unimodal models I–VII were based on individual features. (9) Multimodal models VIII–XIV were based on different combinations of EEG and fMRI features (results shown in Table 3). (10) Finally, pairwise comparisons of the same-sample models were performed, with both machine-learning algorithms, separately (results given in Supplementary Figs 3 and 4). Figure created with BioRender.com.

Box 1); (ii) <31 days from brain injury; and (iii) clinical indication for structural MRI. We aimed to perform clinical exams, EEG and fMRI within a 24-h window. In 26 patients this time window was exceeded due to rescheduling of MRI scans. We aimed for unsedated patients during neurological examinations, EEG and fMRI, but if patients could not fully be weaned from sedation, dosages were reduced to the lowest possible level. Levels of sedation were graded as: 'None or minimal', indicating absence of intravenous fentanyl, remifentanil, propofol, midazolam, sodium thiopental or sevoflurane; 'low to moderate', indicating fentanyl <500 μg/h or <200 μg/h

combined with propofol, remifentanil <1000 µg/h or <250 µg/h combined with propofol, propofol <100 mg/h, midazolam <10 mg/h, sevoflurane <3%; 'high or very high', indicating propofol ≥100 mg/h, fentanyl ≥500 µg/h or ≥200 µg/h combined with propofol, remifentanil ≥1000 µg/h or ≥250 µg/h combined with propofol, midazolam ≥10 mg/h, sevoflurane ≥3% or any dosage of sodium thiopental.[22]

Exclusion criteria were (i) contraindications for MRI; (ii) acute life-threatening conditions with immediate risk of deterioration; (iii) major premorbid neurological deficits, e.g. mental retardation, aphasia or deafness; and (iv) lack of Danish or English language proficiency.

Data acquisition

Clinical data

Demographic and clinical data were obtained during clinical routine, supplemented by electronic health records and recorded in a REDCap database.[23] Patients were classified according to consciousness levels by a detailed neurological bedside examination, performed by or under supervision of an experienced board-certified neurologist (D.K.), as close to the time of fMRI/EEG as possible (i.e. study enrolment), and repeated prior to discharge or death in the ICU, as described earlier[19,24,25] (Supplementary Box 1). Consciousness levels of patients who underwent WLST were determined prior to the initiation of palliative care. Daily neurological assessments were also performed by the attending physicians. The neurological exam included: (i) assessment of cranial nerves and sensorimotor status; (ii) Glasgow Coma Scale (GCS)[26]; (iii) Full Outline of UnResponsiveness (FOUR) score[27]; (iv) visual pursuit/fixation with a mirror; (v) ability to follow simple motor commands (including with the family, when possible, to stimulate arousal); (vi) reaction to central and peripheral noxious stimuli (in the absence of command following); and (vii) assessment of verbal and non-verbal communication.

EEG

Bedside video-EEG was recorded by experienced EEG technicians using a standard 19/25 EEG channel system (NicoletOne, Natus Medical Inc.) according to the international 10–20 system.[28] Artefacts including muscular activity and electronic noise from ICU devices were reduced using standard clinical procedures.

Resting and stimulus-based EEG recording

Recordings included a minimum of 10-min resting-state EEG, during which the surrounding environment was kept quiet. To assess EEG reactivity, patients were evaluated by easy-to-apply stimuli, each of 15 s duration, consisting of (i) passive eye-opening; (ii) pressure applied to both earlobes (to reduce muscle artefacts); (iii) noxious stimuli to fingertips and sternum; (iv) auditory stimulation, calling patients by their name; and (v) tactile sensory stimuli applied with a cotton swab to the nostrils. All stimuli were repeated at least once with a pause of at least 60 s.

Functional MRI

Resting-state fMRI was performed on 1.5 or 3 T MRI-scanners (Siemens) with 20- or 64-channel head coils, respectively. Patients were monitored by experienced neuroanaesthesiologists, unsedated or sedated, if necessary, with sevoflurane or propofol at the lowest possible dosages, to limit movement artefacts. Patients were mechanically ventilated, aiming for normocapnia. Participants completed a 10-min resting-state scan session with T_2^*-weighted echo-planar imaging blood oxygen level-dependent (BOLD) fMRI sequence (repetition time = 2000 ms, echo time = 30 ms, flip angle = 90°, in-plane matrix 64 × 64, number of slices = 32, slice thickness = 3 mm (0.75 mm gap), in-plane resolution = 3.6 × 3.6, iPAT acceleration factor = 2). A high-resolution 3D T_1-weighted structural image was acquired using a sagittal, magnetization-prepared rapid gradient echo (MP-RAGE) sequence (repetition time/echo time/inversion time = 1900/2.58/900 ms, flip angle = 9°, in-plane matrix 256 × 256, number of slices = 224, voxel size = 0.9 × 0.9 × 0.9 mm). A gradient-echo field map of the same spatial dimensions as the BOLD fMRI sequence was acquired to resolve spatial distortions due to magnetic field inhomogeneities (repetition time = 400 ms, echo times = 4.92 and 7.38 ms).

Predictive models

Features

Visual assessment and Synek scale

EEG recordings were visually assessed by two experienced board-certified electroencephalographers (A.S., M.C.) blinded to clinical information, following current international terminology.[29–31] EEG was assessed for (i) best background activity; (ii) continuity and percentage of EEG suppression (i.e. amplitude <10 µV); (iii) presence of posterior dominant rhythm; (iv) periods of low voltage background activity; (v) sleep patterns; (vi) periodic discharges; (vii) epileptiform activity according to 'standardized computer-based organized reporting of EEG'[30]; (viii) status epilepticus according to Salzburg criteria[32]; (ix) presence and type of burst suppression; (x) reactivity to external stimuli[33]; and (xi) overall EEG impression, rated using the Synek scale from I to IV[34]; Supplementary Box 2 provides details. The electroencephalographers evaluated EEGs first separately, then together. Disagreements were resolved by a third board-certified electroencephalographer (M.F.: $n = 15$), also blinded to clinical information.

ABCD spectral categorization

We used the ABCD spectral classification developed by Forgacs *et al.*,[35] where 'A' indicates complete loss of corticothalamic integrity, 'B' and 'C' represent interim regimes with distinct physiological foundations and 'D' indicates full recovery of corticothalamic integrity. EEG segments were identified around times of maximal arousal, e.g. after external stimuli. EEG segments with artefacts from eye blinks, movement or ICU equipment were disregarded. Centrally located channels (Cz, C3, C4, Pz, P3, P4) were chosen for spectral analysis to avoid artefacts from temporal and frontal channels. For quantitative analysis, we selected at least 10 epochs of 10-s, artefact-free EEG per patient. The EEG was re-referenced to the Laplacian montage[36] and bandpass filtered 0.5–40 Hz. We used Thomson's multitaper method[37] for spectral estimation. Results were averaged across epochs for each patient. Analyses were done using MATLAB (version 2018a, Mathworks, Massachusetts, USA). Spectral profiles of EEGs were randomly shuffled, and investigators were blinded to the clinical characteristics. Initially, M.A. and I.Z. visually inspected the spectral profile of each electrode and assigned each to the categories of the 'ABCD' model.[35] EEG spectral features that could not be categorized according to the ABCD model were deemed 'non-ABCD'. A third investigator (D.K.) resolved disagreements ($n = 31$).

EEG markers

We computed a set of 68 EEG markers from the epoched data as described earlier,[38] without the event-related markers from the auditory task: spectral power (raw and normalized) in delta, theta, alpha, beta and gamma, spectral summaries (four markers), weighted symbolic mutual information, permutation entropy and Kolmogorov complexity. Each marker was reduced to four scalar values, comprising mean and standard deviation (SD) across trials and electrodes (four combinations). The markers were computed from resting-state EEG, during stimulation, and combined periods (referred to as 'EEG markers R', 'EEG markers S' and 'EEG markers C', respectively, throughout the article).

Support Vector Machine classifier

The Support Vector Machine (SVM) classifier was developed as described earlier.[38,39] EEG data were first cleaned by an automated procedure. Due to the different montages used in our population, we selected the electrodes closest to the low-density systems (19 and 25 channels). Low-density data from our population were then epoched following the structure of the task-based data before the event-related response (800 ms epochs, 200 ms baseline, random inter-epoch interval between 550 and 850 ms).[40] The 68 EEG markers described above were then used as features in a predictive model. We fed these data into a predictive model that first standardized the features (z-score), selected 20% of the features based on univariate ANOVA f-values, and trained an SVM classifier (linear kernel, grid-searched C [1e-4, 1e-3, e-2, 1e-1, 1, 1e1, 1e2]). We computed the probability of being ≥MCS [$P(\text{MCS}) > 0.5$] using Platt's scaling.[41] We used both resting-state EEG segments and stimulus-based EEG segments separately to determine $P(\text{MCS})$ for each patient, i.e. $P(\text{MCS})_{\text{rest}}$ and $P(\text{MCS})_{\text{stim}}$.

Functional MRI functional connectivity

Resting-state fMRI data were preprocessed using SPM12 (https://www.fil.ion.ucl.ac.uk/spm/software/spm12/) in MATLAB v2019a. Preprocessing steps included realignment and unwarping spatial distortions in the functional volumes; co-registration of functional and structural volumes; segmentation of the structural volume into grey matter, white matter and CSF probability maps; normalization of functional volumes into Montreal Neurological Institute space based on warping parameters estimates during segmentation; and spatial smoothing of functional volumes [8 mm full-width at half-maximum (FWHM) kernel]. Additional processing and denoising was performed in Conn v17c (https://web.conn-toolbox.org/). This included band-pass filtering (0.008–0.09 Hz); regressing motion parameters (and their first derivatives); an estimation of noise sources using anatomical component correction (aCompCor), i.e. regressing out the time series (and first derivative) of the first five principal components from a decomposition of the time series from white matter and CSF voxels, separately.[42] Scans were visually inspected to check data quality and document morphological abnormalities. Six resting-state networks [default mode network (DMN), frontoparietal network (FPN), auditory network (AN), salience network (SN), sensorimotor network (SMN) and visual network (VN)] were defined comprising 42 regions delineated in an *a priori* atlas previously applied to similar clinical cohorts.[43] Denoised regional time series were extracted and region-to-region functional connectivity (FC) was estimated by calculating the time-wise correlation coefficient (Pearson's rho) between each pair of regional time series and applying Fisher's *r*-to-*z* transformation to the correlation coefficient [i.e. $r\text{-to-z} = 0.5 \times (\ln((1+r)/(1-r)))$], where r is the correlation coefficient and ln represents the natural logarithm). Within- and between-network functional connectivity was calculated as the average functional connectivity across the set of respective region-to-region pairs (FC).

Targets

DoC status from two time points was used as the target of classification models: time of study enrolment ($\text{DoC}_{\text{enrolment}}$) and time of ICU discharge or death ($\text{DoC}_{\text{discharge}}$). Patients were dichotomously classified as (i) clinically unconscious, i.e. in a coma/UWS (≤UWS); or (ii) MCS– or better (≥MCS).

Machine-learning algorithms

We used two different machine-learning algorithms: an SVM with a linear kernel and a Random Forest.[44] We used nested cross-validation (stratified k-fold, $k = 5$) to ensure that within-fold class ratio was representative of the entire dataset. Grid search was used to select the SVM hyperparameter, C (values: 0.0001, 0.001, 0.01, 0.1, 1, 10, 100). The Random Forest hyperparameters were set at 500 trees per forest and sqrt(p) features per tree, where p is the number of predictive features. Before input to the SVM learning algorithm, the data were transformed using a z-score (learnt only on the training sets). In the case of EEG markers, where the features were computed from either 19 or 25 electrode systems, the data were de-confounded for the number of electrodes using a linear regression.

Model evaluation

We assessed prediction performance of EEG and fMRI features with area under the curve (AUC) of receiver operating characteristic (ROC) curves, sensitivity and positive predictive value. Model performance with AUC > 0.50 indicated that the respective model could predict target outcome above chance level. Sensitivity and positive predictive value were graded (arbitrarily) as low (<0.65), moderate (0.65–0.70) or high (>0.70). Our primary outcome was the ability of EEG and MRI to classify consciousness level (i.e. ≤UWS or ≥MCS) at the time of enrolment. Our secondary outcome was the ability of EEG and fMRI to predict consciousness level at ICU discharge. For sensitivity and positive predictive value, we considered ≥MCS as the positive and ≤UWS as the negative outcomes. Accordingly, we calculated the positive predictive value (i.e. the fraction of patients with good outcome among those with predicted good outcome according to the model) and the sensitivity (i.e. the fraction of all patients with good clinical outcome that were predicted by the model to have good outcome):

$$\begin{aligned} \textit{positive predictive value} &= \textit{precision} = \frac{TP}{TP + FP} \\ \textit{sensitivity} &= \textit{recall} = \frac{TP}{TP + FN} \end{aligned} \quad (1)$$

where TP indicates the number of patients with a 'true positive', FP those with a 'false positive', and FN those with a 'false negative' prediction, respectively.

We performed stratified 5-fold cross validation with 100 repetitions. Performance of each repetition was computed as the mean of performance estimates across the five folds; overall model

performance was computed as mean performance across all 100 repetitions.

Statistical analysis

Quantitative data are expressed as mean ± SD or median (range) and were compared between groups with Student's *t*-test, Mann–Whitney U-test, or Kruskal–Wallis test. Categorical data are expressed as *n* (percentages) and compared using chi-squared test or Fisher's exact test. Some group difference estimates, e.g. resting-state network connectivity, are reported as Cohen's *d*. Unadjusted *P*-values <0.05 were considered statistically significant. Unless otherwise stated, AUC, positive predictive value and sensitivity estimates are reported as mean value; 95% CI.

Ethics

This study was approved by The Danish Data Protection Agency (RH-2016-191, I-Suite nr:04760) and the Ethics Committee of the Capital Region of Denmark (File-nr.:H-16040845). Written consent was waived because all data were acquired during routine clinical work-up (including fMRI, during clinically indicated MRI). 'CONNECT-ME' is registered with clinicaltrials.org (NCT02644265).

Data and code availability

Data from fMRI cannot be made anonymous and are not publicly available. Other data will be shared upon reasonable request. The code used in the predictive models is available at https://github.com/fraimondo/connect-me. All analysis was done using Julearn and scikit-learn.[45]

Results

Clinical data

The final study population consisted of 87 patients [mean age 50 ± 18.7 years; 37 females (42.5%); 77 (88.5%) patients with baseline modified Rankin Scale score ≤2, Table 1]. Cause of admission was TBI in 25 patients (29.1%), ischaemic stroke in 11 (12.8%), subarachnoid or intracerebral haemorrhage in 11 (12.8%), cardiac arrest in 10 (11.6%), epilepsy in five (5.8%) and other medical or neurological disorders in 25 (29.1%) patients. Thirty-six patients (41.4%) had highly pathological neuroimaging at admission (Table 1). Median length of stay in the ICU was 27 days, and the median length of hospital stay 33 days. On average, coma/UWS patients stayed in the ICU for as many days as patients who were MCS or better (Table 1 and Supplementary Table 1). Thirty-one patients (35.6%) died in the ICU, of whom 29 were classified as coma/UWS at enrolment; 28 patients had life-sustaining therapy withdrawn (Table 1). Length of ICU admission was significantly longer in patients discharged from the ICU alive (mean 36.8 ± 27.9 days) compared to those who died (mean 21.9 ± 14.2 days). EEG recordings were available from 86 patients and fMRI from 64 patients (Fig. 1).

Clinical consciousness levels according to $DoC_{enrolment}$ were: coma in 24 (27.5%), UWS in 27 (31.4%), MCS– in 19 (21.8%), MCS+ in 10 (11.5%), LIS in 5 (5.7%) and eMCS/CS in 2 (2.3%) patients (Fig. 2). Supplementary Table 2 shows behavioural and clinical details for individual patients.

EEG features and consciousness levels

Synek scale

EEGs ($n = 86$) were graded according to the Synek scale (I–V, best to worst EEG activity) as follows: I, 18 (20.9%); II, 44 (51.2%); III, 15 (17.4%); IV, 6 (7.0%); and V 3 (3.5%). $DoC_{enrolment}$ and $DoC_{discharge}$ were both predicted by Synek grade, using the Random Forest model ($DoC_{enrolment}$: AUC = 0.79; 0.77–0.80, $DoC_{discharge}$: AUC = 0.71; 0.66–0.74), with high positive predictive value but low sensitivity (Table 2). The SVM model predicted $DoC_{enrolment}$ (AUC = 0.70; 0.68–0.71), but not $DoC_{discharge}$ (AUC = 0.56; 0.46–0.65); Fig. 3 and Table 2 show details.

ABCD spectral categories

EEG grading into ABCD spectral categories (i.e. A–D, from least preserved to fully preserved corticothalamic integrity) was possible for 73 patients (84.9%): 'A', 35 (40.7%); 'B', 28 (32.6%); 'C', two (2.3%); and 'D' eight (9.3%). EEG from 13 patients (15.1%) did not fit with ABCD categories ('non-ABCD'). Supplementary Fig. 1 shows examples from each ABCD category. The Random Forest model predicted $DoC_{enrolment}$ and $DoC_{discharge}$ using ABCD categories ($DoC_{enrolment}$: AUC = 0.64; 0.58–0.68; $DoC_{discharge}$: AUC = 0.58; 0.56–0.61), although with low/moderate positive predictive value and low sensitivity (Table 2). SVM model predicted $DoC_{enrolment}$ (AUC = 0.61; 0.52–0.54) with low positive predictive value and sensitivity but could not predict $DoC_{discharge}$ (AUC = 0.58; 0.46–0.64) (Fig. 3 and Table 2).

EEG markers

EEG markers could be extracted from 85 resting-state EEG segments and 77 EEG segments with external stimuli. We report AUCs for the Random Forest model here, but Table 2 shows all AUC, positive predictive value and sensitivity estimates. From the three sets of features (EEG markers R, S and C), only EEG markers S and C predicted $DoC_{enrolment}$ (markers S: AUC = 0.62; 0.54–0.67; markers C: AUC = 0.60; 0.52–0.66), although with low positive predictive value and sensitivity. All three sets of features predicted $DoC_{discharge}$ (EEG markers R: AUC = 0.71; 0.63–0.76; markers S: AUC = 0.66; 0.59–0.72; markers C: AUC = 0.71; 0.64–0.76) with a moderate positive predictive value and high sensitivity (Fig. 3 and Table 2).

Support Vector Machine classifier

Both $P(MCS)_{Rest}$ and $P(MCS)_{Stim}$ are the output of a predictive SVM classifier trained on a separate dataset[38] and tested on the EEG markers R and S data. Both $P(MCS)_{Rest}$ and $P(MCS)_{Stim}$, when used as features, predicted $DoC_{enrolment}$ using the Random Forest model (AUC = 0.63; 0.55–0.70) and the SVM model (AUC = 0.64; 0.54–0.69), with low positive predictive value and sensitivity (Table 2). $DoC_{discharge}$ was only predicted with the SVM model (AUC = 0.69; 0.62–0.75) with low positive predictive value but high sensitivity (Fig. 3 and Table 2).

Functional MRI functional connectivity and consciousness levels

We evaluated associations and predictions based on resting-state fMRI within-network and between-network connectivity estimates across 64 patients with available data (Figs 3 and 4, Table 2 and Supplementary Table 3).

Compared to patients classified as ≥MCS at enrolment (Fig. 4A and Supplementary Table 3), mean network connectivity in

Table 1 Clinical characteristics and comparison between patients in coma or UWS (≤UWS) versus patients in MCS− or better (≥MCS)

	Total ($n = 87$)	≥MCS ($n = 36$)	≤UWS ($n = 51$)	OR (95% CI)	P
Age, year, mean (SD)	50 (18.7)	47 (17.0)	52.2 (19.8)	–	0.19
Sex, female, *n* (%)	37 (42.5)	16 (44.4)	21 (41.2)	0.88 (0.37–2.10)	0.93
mRS baseline, *n* (%)					
0–2	77 (88.5)	32 (88.9)	45 (88.2)	0.95 (0.22–3.7)	1.00
>2	10 (11.5)	4 (11.1)	6 (11.8)	Reference	–
History of comorbidity, any, *n* (%)[a]	63 (72.4)	23 (63.9)	40 (78.4)	2.03 (0.78–5.42)	0.15
Cardiopulmonary	34 (39.0)	10 (27.8)	24 (47.1)	2.28 (0.92–5.91)	0.11
Neurological disorders					
Cerebrovascular	11 (12.6)	5 (13.9)	6 (11.8)	0.82 (0.22–3.19)	0.76
Epilepsy	7 (8.0)	4 (11.1)	3 (5.9)	0.51 (0.09–2.59)	0.44
Other	18 (20.7)	9 (25.0)	9 (17.6)	0.65 (0.22–1.88)	0.57
Diabetes	10 (11.5)	4 (11.1)	6 (11.8)	1.05 (0.27–4.60)	1.00
Psychiatric disorders, any	14 (16.1)	6 (16.7)	8 (15.7)	0.94 (0.29–3.15)	1.00
Other medical or surgical comorbidities	37 (42.5)	13 (36.1)	24 (47.1)	1.56 (0.65–3.83)	0.43
Cause of ICU admission, *n* (%)					
TBI	25 (28.7)	10 (27.8)	15 (29.4)	1.08 (0.42–2.87)	1.00
Ischaemic stroke	11 (12.6)	6 (16.7)	5 (9.8)	1.82 (0.49–7.05)	0.51
Cardiac arrest	10 (11.5)	0 (0)	10 (19.6)	–	<0.01*
Subarachnoid haemorrhage	6 (6.9)	4 (11.1)	2 (3.9)	0.34 (0.04–1.97)	0.23
Intracerebral haemorrhage	5 (5.7)	2 (5.6)	3 (5.9)	0.96 (0.11–6.65)	1.00
Epilepsy, including status epilepticus	5 (5.7)	2 (5.6)	3 (5.9)	0.96 (0.11–6.65)	1.00
Other causes, neurology[b]	16 (18.4)	10 (27.8)	6 (11.8)	0.35 (0.11–1.08)	0.11
Other causes, medical or surgical[c]	9 (10.3)	2 (5.6)	7 (13.7)	2.55 (0.56–6.65)	0.30
Highly pathological[d] neuroimaging, *n* (%)	36 (41.4)	13 (36.1)	23 (45.1)	1.44 (0.60–3.55)	0.54
GCS score index, median (range)	6 (3–14)	9 (4–14)	5 (3–9)	0.36 (0.24–0.55)	<0.01*
FOUR score index, median (range)	8 (0–16)	11.5 (5–16)	6 (0–10)	0.35 (0.22–0.57)	<0.01*
Brain injury to ICU admission, days, median (range)	0 (0–19)	0 (0–19)	0 (0–16)	0.90 (0.79–1.04)	0.04*
ICU admission to enrolment, days, median (range)	11 (1–54)	11 (1–54)	10.5 (1–31)	0.97 (0.94–1.01)	0.44
Time between EEG and fMRI, h, median (range)	3.8 (0.3–216)	20 (0.3–216)	3.2 (1.0–190)	0.99 (0.98–1.00)	0.08
Level of sedation[e] during clinical exam, *n* (%)					0.17
None or minimal	59 (67.8)	27 (75.0)	32 (62.8)	Reference	–
Low to moderate	19 (21.8)	8 (22.2)	11 (21.6)	1.15 (0.40–3.43)	0.80
High or very high	9 (10.3)	1 (2.8)	8 (15.7)	5.93 (0.97–156)	0.06
Level of sedation[e] during EEG, *n* (%)	86	36	50		0.72
None or minimal	62 (71.3)	27 (75.0)	35 (70.0)	Reference	–
Low to moderate	16 (18.6)	7 (19.4)	9 (18.0)	0.99 (0.32–3.15)	0.98
High or very high	8 (9.2)	2 (5.6)	6 (12.0)	2.19 (0.45–17.6)	0.35
Level of sedation[e] during fMRI, *n* (%)	64	29	35		0.10
None or minimal	23 (36.0)	6 (20.7)	17 (48.6)	Reference	–
Low to moderate	21 (32.8)	11 (37.9)	10 (28.6)	0.33 (0.09–1.17)	0.09
High or very high	18 (28.2)	10 (34.5)	8 (22.9)	0.29 (0.07–1.09)	0.07
Unknown	2 (3.1)	2 (6.9)	0 (0)	–	–
Duration of ICU admission, days, median (range)	27 (0–160)	25 (0–160)	27 (2–119)	–	0.72
Duration of hospital admission, days, median (range)	33 (2–160)	37.5 (10–160)	32 (2–129)	–	0.09
Death during ICU admission, *n* (%)	31 (35.6)	2 (5.6)	29 (56.9)	20.4 (5.34–147)	<0.01*
Withdrawal of life-sustaining therapy	28 (32.2)	1 (2.8)	27 (52.9)	11.2 (0.23–536)	0.19
Sudden clinical deterioration	3 (3.4)	1 (2.8)	2 (3.9)	–	–

[a]Some patients had multiple comorbidities.
[b]Other causes, neurology included: autoimmune encephalitis ($n = 4$), brain tumour ($n = 3$), hydrocephalus and shunt revision ($n = 2$), meningoencephalitis ($n = 2$), global cerebral oedema ($n = 2$), cerebral venous thrombosis ($n = 1$), myasthaenic crisis ($n = 1$) and anoxic ischaemic brain damage due to drowning ($n = 1$).
[c]Other causes, medical or surgical included: hypo- or hyperglycaemia ($n = 2$), acute respiratory failure ($n = 2$), aortic dissection or ruptured aortic aneurysm ($n = 2$), perforated diverticulitis ($n = 1$), pulmonary embolism ($n = 1$) and carbon monoxide poisoning.
[d]Highly pathological findings on neuroimaging were defined as Fisher grade ≥3 (for subarachnoid haemorrhage), Marshall classification ≥3 (for TBI), haemorrhage volume ≥30 ml (for intracerebral haemorrhage), strategic haemorrhage or infarct in brainstem (for ischaemic stroke or infratentorial haemorrhage), any visible sign of anoxic brain injury on CT scan (for cardiac arrest), global cortical oedema (for patients with brain oedema), brain tumours with midline compression, compression of basal cisterns and/or visible signs of hydrocephalus (for patients with any type of brain tumour).
[e]See the 'Materials and methods' section for details sedation levels.
*Statistically significant *P*-values.

≤UWS patients was lower in DMN–DMN ($P = 0.007$) and SMN–VN ($P = 0.006$), and higher in DMN–VN ($P = 0.034$), FPN–AN ($P = 0.009$) and SN–SMN ($P = 0.047$). Similarly, patients classified as ≤UWS at ICU-discharge (Fig. 4B) had lower mean network connectivity in DMN–DMN ($P = 0.001$), VN–VN ($P = 0.010$), FPN–VN ($P = 0.049$) and SMN–VN ($P = 0.030$) when compared to patients classified as ≥MCS at ICU discharge, but network effects did not remain statistically significant after Bonferroni correction.

The set of within- and between-network connectivity estimates predicted $DoC_{enrolment}$, using the Random Forest model (AUC = 0.75;

Table 2 Prediction performance EEG- and fMRI features in predicting consciousness levels at study enrolment and ICU discharge

Model	Features	Study enrolment			ICU discharge		
		AUC	Positive predictive value	Sensitivity	AUC	Positive predictive value	Sensitivity
Random Forest	Synek	0.79 [0.77 0.80][a]	0.74 [0.63 0.81][a]	0.54 [0.45 0.64]	0.71 [0.66 0.74][a]	0.83 [0.70 0.90][a]	0.56 [0.54 0.61]
	ABCD	0.64 [0.58 0.68]	0.53 [0.38 0.63]	0.56 [0.38 0.67]	0.58 [0.56 0.61]	0.67 [0.61 0.74]	0.61 [0.59 0.67]
	EEG markers C	0.60 [0.52 0.66]	0.52 [0.37 0.66]	0.37 [0.27 0.47]	0.71 [0.64 0.76][a]	0.69 [0.64 0.73]	0.76 [0.70 0.82]
	EEG markers R	0.56 [0.47 0.63]	0.49 [0.34 0.61]	0.39 [0.28 0.47]	0.71 [0.63 0.76][a]	0.69 [0.63 0.73]	0.78 [0.71 0.84]
	EEG markers S	0.62 [0.54 0.67]	0.54 [0.39 0.69]	0.42 [0.28 0.50]	0.66 [0.59 0.72]	0.65 [0.61 0.70]	0.74 [0.66 0.82]
	SVM	0.63 [0.55 0.70]	0.47 [0.35 0.59]	0.41 [0.33 0.50]	0.54 [0.46 0.61]	0.55 [0.49 0.62]	0.56 [0.48 0.63]
	fMRI FC	0.75 [0.67 0.82]	0.67 [0.54 0.77]	0.60 [0.48 0.70][a]	0.64 [0.58 0.72]	0.68 [0.64 0.72]	0.85 [0.78 0.90][a]
SVM	Synek	0.70 [0.68 0.71]	0.76 [0.52 0.93][a]	0.40 [0.22 0.59]	0.56 [0.46 0.65]	0.60 [0.58 0.61]	0.97 [0.90 1.00][a]
	ABCD	0.61 [0.52 0.64]	0.05 [0.00 0.17]	0.03 [0.00 0.10]	0.58 [0.46 0.64]	0.58 [0.54 0.59]	0.94 [0.86 1.00]
	EEG markers C	0.61 [0.53 0.68]	0.31 [0.12 0.54]	0.27 [0.10 0.47]	0.63 [0.54 0.72]	0.64 [0.56 0.72]	0.68 [0.56 0.82]
	EEG markers R	0.60 [0.50 0.69]	0.42 [0.21 0.60]	0.35 [0.18 0.52]	0.68 [0.60 0.78]	0.69 [0.63 0.76][a]	0.73 [0.61 0.86]
	EEG markers S	0.64 [0.54 0.72]	0.43 [0.20 0.68]	0.33 [0.17 0.50]	0.60 [0.51 0.67]	0.62 [0.54 0.71]	0.69 [0.57 0.81]
	SVM	0.64 [0.54 0.69]	0.18 [0.04 0.34]	0.18 [0.03 0.35]	0.69 [0.62 0.75][a]	0.61 [0.56 0.65]	0.82 [0.75 0.91]
	fMRI FC	0.71 [0.62 0.81][a]	0.64 [0.46 0.76]	0.57 [0.39 0.70][a]	0.66 [0.56 0.76]	0.68 [0.62 0.76]	0.88 [0.71 1.00]

Prediction performance is based on $n_{max} = 86$, see the 'Materials and methods' section and Fig. 1, step 7. Values in square brackets are 95% CI. EEG markers C = 68 EEG markers derived from the full EEG recording; EEG markers R = 68 EEG markers derived from EEG segments with resting state recordings; EEG markers S = 68 EEG markers derived from EEG segments with stimulations; SVM = Support vector machine classifier indicating probability of consciousness derived from EEG markers R and S.
[a]The highest AUCs, positive predictive values and sensitivities obtained for prediction of consciousness level at enrolment and discharge depending on the learning algorithm.

0.67–0.82) and the SVM model (AUC = 0.71; 0.62–0.81), with moderate to low positive predictive value and low sensitivity (Table 2). The same features were also predicted $DoC_{discharge}$ using the Random Forest model (AUC = 0.64; 0.58–0.72) and the SVM model (AUC = 0.66; 0.56–0.76), with moderate positive predictive value but high sensitivity (Fig. 3 and Table 2).

Model comparisons

To compare the model performances without bias regarding the features used, we benchmarked the models using the same sample set (i.e. $n = 48$ patients with all data available), the same train/test split for each repetition of the stratified 5-fold cross validation and computed the difference in metrics between the individual folds. Here, we report results from the Random Forest models; Table 3 shows results from all same-sample models.

Overall, the results for the unimodal models were maintained, but we observed higher variance across folds, an expected behaviour after reducing the amount of samples to train the models (Fig. 3C and D). Using either Random Forest or SVM learning algorithms, all models except the model based on ABCD categories were able to predict $DoC_{enrolment}$ and $DoC_{discharge}$ above chance level (Table 2 and Fig. 3C–E). Pairwise comparison of the models (Supplementary Figs 2 and 3) shows that all unimodal models (I, III to VII) had similar performance, except for the ABCD model (II) at $DoC_{discharge}$, which performed worse (Supplementary Figs 2B and 3B).

Combining EEG and functional MRI features to predict consciousness levels

We evaluated prediction of consciousness levels of patients with all EEG and resting-state fMRI connectivity measures available ($n = 48$). The median time between clinical exam, EEG and fMRI was <4 h (Table 1). We tested several models combining the different EEG and fMRI features (Fig. 3D and F; models VIII to XIV), achieving above-chance level accuracy with both machine-learning algorithms (Table 3). The highest AUCs for predicting $DoC_{enrolment}$ were obtained with Random Forest using fMRI FC and EEG markers S (Model X; AUC = 0.78; 0.71–0.86) as well as fMRI FC, ABCD, SVM and Synek (Model XI; AUC = 0.78; 0.68–0.84). With the SVM algorithm, the highest AUC for $DoC_{enrolment}$ was obtained using the SVM model classifications as features (Model VI; AUC = 0.78; 0.72–0.83). For $DoC_{discharge}$, the highest AUCs using the Random Forest algorithm was obtained with EEG markers C (Model III; AUC = 0.81; 0.74–0.88), EEG markers R (Model IV; AUC = 0.81; 0.74–0.88) and ABCD, SVM, Synek and EEG markers C (Model XIII; AUC = 0.81; 0.74–0.88). With the SVM algorithm, the highest AUC was obtained using fMRI FC and EEG markers R (AUC = 0.83; 0.75–0.89).

Same sample models were repeated after excluding patients who died due to WLST. However, the performance of these models was not satisfactory because of the substantially reduced dataset ($n = 35$). Results are presented in Supplementary Table 4.

Patients with discrepancy between EEG/functional MRI characteristics and consciousness level

Complete EEG features [i.e. Synek category, ABCD category and SVM classifier-derived P(MCS)] were available from 40 of 51 ≤UWS patients. In 11 (27.5%) we found a disconnect between their unresponsiveness at $DoC_{enrolment}$ and their favourable EEG scores [i.e. a combination of Synek I or II, ABCD model categories B, C, or D and P(MCS) >0.50]. Supplementary Table 5 shows characteristics of these patients. Comparison of ≤UWS patients with and without favourable EEG features revealed no differences in terms of outcome or other clinical characteristics.

FMRI data were available from 32 (80%) of the 40 ≤UWS patients with complete EEG features. Comparing fMRI resting-state network connectivity in ≤UWS patients ($n = 8$) with favourable EEG features to the ≤UWS patients ($n = 24$) with unfavourable EEG features, we found that the overall between-network connectivity was

Table 3 Prediction performance of same-sample EEG- and fMRI features in predicting consciousness levels at study enrolment and ICU discharge

Model	Features	Study enrolment			ICU discharge		
		AUC	Positive predictive value	Sensitivity	AUC	Positive predictive value	Sensitivity
Random Forest	I: Synek	0.74 [0.64 0.78]	0.70 [0.50 0.86]	0.49 [0.41 0.58]	0.71 [0.62 0.75]	0.68 [0.59 0.77]	0.73 [0.58 0.92]
	II: ABCD	0.65 [0.60 0.68]	0.52 [0.33 0.65]	0.50 [0.33 0.67]	0.53 [0.40 0.59]	0.61 [0.56 0.63]	0.91 [0.73 1.00][a]
	III: EEG markers C	0.71 [0.62 0.77]	0.66 [0.51 0.79]	0.60 [0.51 0.69]	0.81 [0.74 0.88][a]	0.77 [0.72 0.83]	0.82 [0.77 0.87]
	IV: EEG markers R	0.62 [0.54 0.71]	0.53 [0.36 0.68]	0.47 [0.38 0.54]	0.81 [0.74 0.88][a]	0.79 [0.72 0.86][a]	0.79 [0.73 0.87]
	V: EEG markers S	0.75 [0.67 0.81]	0.74 [0.63 0.84]	0.65 [0.56 0.72][a]	0.74 [0.67 0.82]	0.76 [0.69 0.82]	0.81 [0.73 0.87]
	VI: SVM	0.69 [0.58 0.78]	0.63 [0.48 0.77]	0.58 [0.46 0.67]	0.68 [0.61 0.77]	0.72 [0.66 0.78]	0.75 [0.63 0.87]
	VII: fMRI FC	0.75 [0.66 0.83]	0.69 [0.51 0.80]	0.56 [0.45 0.68]	0.70 [0.61 0.77]	0.66 [0.60 0.71]	0.78 [0.70 0.83]
	VIII: fMRI FC, EEG markers C	0.73 [0.65 0.79]	0.66 [0.52 0.80]	0.59 [0.48 0.67]	0.80 [0.73 0.87]	0.76 [0.69 0.82]	0.81 [0.77 0.87]
	IX: fMRI FC, EEG markers R	0.67 [0.59 0.75]	0.55 [0.39 0.68]	0.48 [0.38 0.58]	0.80 [0.74 0.87]	0.77 [0.69 0.84]	0.79 [0.72 0.87]
	X: fMRI FC, EEG markers S	0.78 [0.71 0.86][a]	0.76 [0.63 0.88][a]	0.64 [0.52 0.72]	0.75 [0.68 0.81]	0.75 [0.69 0.81]	0.82 [0.77 0.87]
	XI: fMRI FC, ABCD, SVM, Synek	0.78 [0.68 0.84][a]	0.73 [0.57 0.85]	0.57 [0.44 0.68]	0.69 [0.60 0.76]	0.67 [0.61 0.72]	0.78 [0.70 0.83]
	XII: ABCD, SVM, Synek	0.74 [0.65 0.82]	0.69 [0.50 0.81]	0.60 [0.47 0.72	0.68 [0.58 0.76]	0.70 [0.62 0.78]	0.75 [0.62 0.87]
	XIII: ABCD, SVM, Synek, EEG markers C	0.70 [0.63 0.78]	0.66 [0.50 0.79]	0.60 [0.48 0.69]	0.81 [0.74 0.88][a]	0.77 [0.71 0.83]	0.82 [0.77 0.87]
	XIV: fMRI FC, ABCD, SVM, Synek, EEG markers C	0.72 [0.64 0.80]	0.67 [0.51 0.80]	0.59 [0.51 0.67]	0.80 [0.73 0.88]	0.76 [0.70 0.82]	0.81 [0.77 0.87]
SVM	I: Synek	0.66 [0.63 0.69]	0.62 [0.32 0.93]	0.33 [0.12 0.53]	0.62 [0.53 0.67]	0.63 [0.60 0.63]	1.00 [0.92 1.00][a]
	II: ABCD	0.67 [0.65 0.68]	0.52 [0.17 0.80]	0.20 [0.07 0.25]	0.49 [0.42 0.50]	0.63 [0.63 0.63]	1.00 [1.00 1.00][a]
	III: EEG markers C	0.65 [0.54 0.73]	0.50 [0.23 0.74]	0.43 [0.17 0.64]	0.80 [0.69 0.90]	0.82 [0.72 0.91][a]	0.76 [0.65 0.87]
	IV: EEG markers R	0.60 [0.49 0.72]	0.32 [0.07 0.60]	0.23 [0.05 0.41]	0.80 [0.70 0.86]	0.79 [0.71 0.87]	0.76 [0.63 0.85]
	V: EEG markers S	0.71 [0.63 0.78]	0.68 [0.50 0.86]	0.56 [0.37 0.71]	0.67 [0.52 0.79]	0.71 [0.62 0.78]	0.79 [0.67 0.90]
	VI: SVM	0.78 [0.72 0.83][a]	0.72 [0.56 0.80]	0.67 [0.61 0.75][a]	0.81 [0.74 0.87]	0.73 [0.65 0.80]	0.81 [0.77 0.90]
	VII: fMRI FC	0.73 [0.60 0.83]	0.61 [0.36 0.77]	0.53 [0.35 0.70]	0.74 [0.64 0.84]	0.76 [0.66 0.85]	0.76 [0.62 0.87]
	VIII: fMRI FC, EEG markers C	0.66 [0.57 0.75]	0.48 [0.27 0.72]	0.42 [0.21 0.63]	0.81 [0.70 0.89]	0.81 [0.69 0.90]	0.77 [0.67 0.87]
	IX: fMRI FC, EEG markers R	0.61 [0.51 0.70]	0.30 [0.02 0.55]	0.26 [0.02 0.45]	0.83 [0.75 0.89][a]	0.82 [0.74 0.91][a]	0.77 [0.68 0.83]
	X: fMRI FC, EEG markers S	0.75 [0.66 0.83]	0.74 [0.53 0.91][a]	0.58 [0.42 0.68]	0.67 [0.58 0.78]	0.68 [0.61 0.77]	0.80 [0.68 0.90]
	XI: fMRI FC, ABCD, SVM, Synek	0.74 [0.62 0.82]	0.57 [0.34 0.75]	0.51 [0.33 0.71]	0.75 [0.61 0.84]	0.76 [0.66 0.84]	0.78 [0.67 0.87]
	XII: ABCD, SVM, Synek	0.72 [0.63 0.81]	0.65 [0.45 0.85]	0.53 [0.38 0.67]	0.73 [0.61 0.82]	0.69 [0.60 0.75]	0.80 [0.70 0.90]
	XIII: ABCD, SVM, Synek, EEG markers C	0.65 [0.57 0.75]	0.52 [0.27 0.78]	0.43 [0.19 0.65]	0.81 [0.67 0.90]	0.82 [0.71 0.92][a]	0.75 [0.63 0.87]
	XIV: fMRI FC, ABCD, SVM, Synek, EEG markers C	0.66 [0.58 0.76]	0.48 [0.25 0.69]	0.39 [0.18 0.60]	0.80 [0.70 0.90]	0.80 [0.69 0.90]	0.76 [0.65 0.87]

Prediction performance is based on $n = 48$; see the 'Materials and methods' section and Fig. 1, steps 8 and 9. Values in square brackets are 95% CI. FC = functional connectivity; EEG markers C = 68 EEG markers derived from the full EEG recording, EEG markers R = 68 EEG markers derived from EEG segments with resting state recordings; EEG markers S = 68 EEG markers derived from EEG segments with stimulations; SVM = Support vector machine classifier indicating probability of consciousness derived from EEG markers R and S.

[a]The highest AUCs, positive predictive values and sensitivities obtained for prediction of consciousness level at enrolment and discharge depending on the learning algorithm.

numerically increased in ≤UWS patients with unfavourable EEG features, whereas within-network DMN connectivity was numerically decreased (Fig. 5), but not statistically significant.

Discussion

Detecting consciousness in clinically unresponsive patients is a major challenge. Predicting which patients will recover consciousness and interact meaningfully with their surroundings is an even more formidable task. Advanced imaging, neurophysiological tools and artificial intelligence might help attain these goals; however, it remains unknown what specific combination of diagnostic tools performs best.

In this prospective, diagnostic phase 2b, ICU cohort study of acute DoC patients, EEG and fMRI performed equally well in distinguishing ≤UWS from ≥MCS patients during ICU admission and in predicting consciousness levels at ICU discharge. However, the performance of the two methodologies differed in positive predictive value and sensitivity. By applying machine learning to a combination of EEG- and fMRI-based features, we obtained lower false positive and false negative rates, indicating opportunities in the ICU to improve prognostication of consciousness recovery.

EEG and consciousness levels

Although pairwise comparison did not show a difference between same-sample models, of the three EEG methods utilized to predict consciousness levels, visual EEG grading with the Synek scale[34] produced the highest AUC (0.79), when tested in a unimodal Random Forest model. That EEGs were analysed by experienced electroencephalographers might explain the strong performance of models based on visual EEG assessments. Our cohort differed in several important aspects from previous cohorts evaluated with the ABCD model (originally based on a homogeneous post-cardiac arrest population[35]) and the SVM classifier (originally based on DoC patients assessed with high-density EEG, including active stimulation[38]). For instance, neuronal underpinnings of acute DoC are likely different from those of chronic DoC; our patient cohort was heterogeneous in disease mechanisms and severity; EEG is subject to artefacts related to ICU equipment, sedation and comorbidities; and clinical EEG has lower spatial resolution than high-density EEG used in the development of the SVM classifier.[38] All these factors may limit the generalizability of the ABCD model and the SVM classifier and reduce performance in our cohort compared to previous reports.[35,38,39,46] Although combining all EEG features in a same-sample model did not increase the overall performance, positive predictive value and sensitivity were indeed improved, despite a markedly decreased sample size ($n = 48$). This indicates that, when different EEG features are available, combining them provides better classification performance, which is important given that EEG is more readily available in the ICU than MRI.

Functional MRI and consciousness levels

DMN connectivity was decreased in ≤UWS compared to ≥MCS patients at enrolment and ICU discharge. This is consistent with previous findings.[47–49] Furthermore, overall between-network connectivity estimates were numerically higher in ≤UWS than in ≥MCS patients. The same pattern has been reported in chronic DoC,[50,51] suggesting that a combination of decreased DMN connectivity and increased between-network connectivity is a prominent feature also in acute DoC, in particular in ≤UWS patients.

Although more patients needed sedation during fMRI than during EEG, fMRI models still predicted consciousness well. Performance of fMRI features in classifying consciousness levels at enrolment and predicting consciousness at ICU discharge was

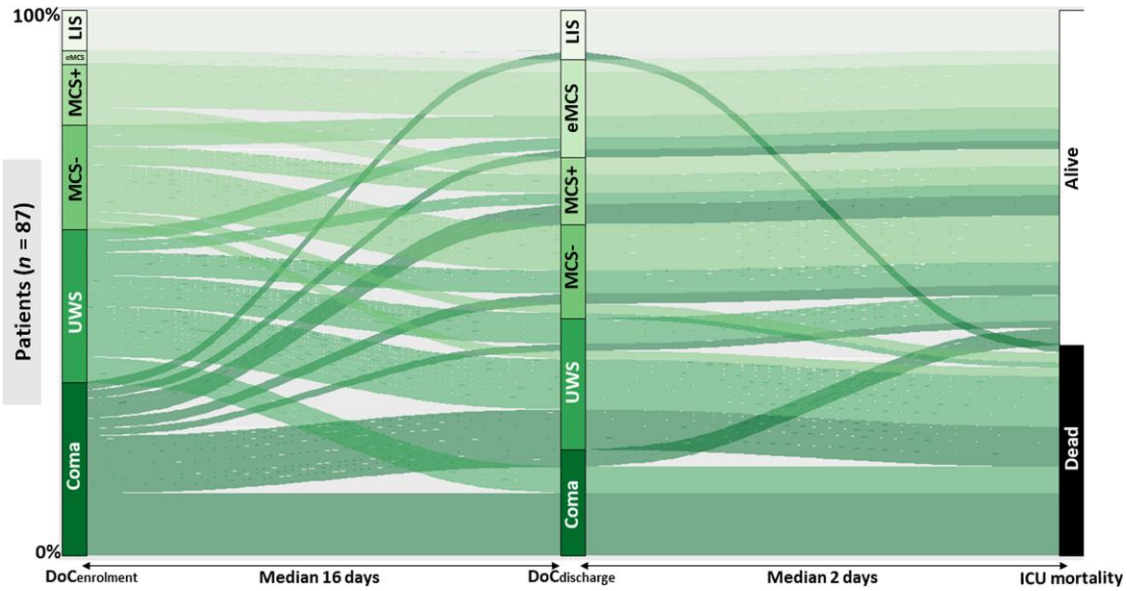

Figure 2 Consciousness levels during ICU admission and relation to mortality in the ICU. Alluvial plot illustrating clinical classification of consciousness level of all patients ($n = 87$) at enrolment ($DoC_{enrolment}$) and at discharge from ICU (alive or dead, $DoC_{discharge}$). Percentages of patients are depicted on the *y*-axis. As illustrated on the *x*-axis, median time between assessment of $DoC_{enrolment}$ and $DoC_{discharge}$ was 16 days, while median time between $DoC_{discharge}$ and death in ICU was 2 days. Distribution of patients according to $DoC_{enrolment}$ was: 24 (27.5%) coma, 27 (31.4%) UWS, 19 (21.8%) MCS−, 10 (11.5%) MCS+, two (2.3%) eMCS/CS and five (5.7%) LIS. Distribution of patients according to $DoC_{discharge}$ was: 16 (18.4%) coma, 20 (23.0%) UWS, 20 (23.0%) MCS−, 11 (12.6%) MCS+, 13 (14.9%) LIS and seven (8.0%) eMCS/CS. In total 31 (35.6%) patients died in the ICU, of whom 28 (90.3%) were classified as coma/UWS at enrolment. In sum, the majority of deaths in ICU occurred in ≤UWS patients.

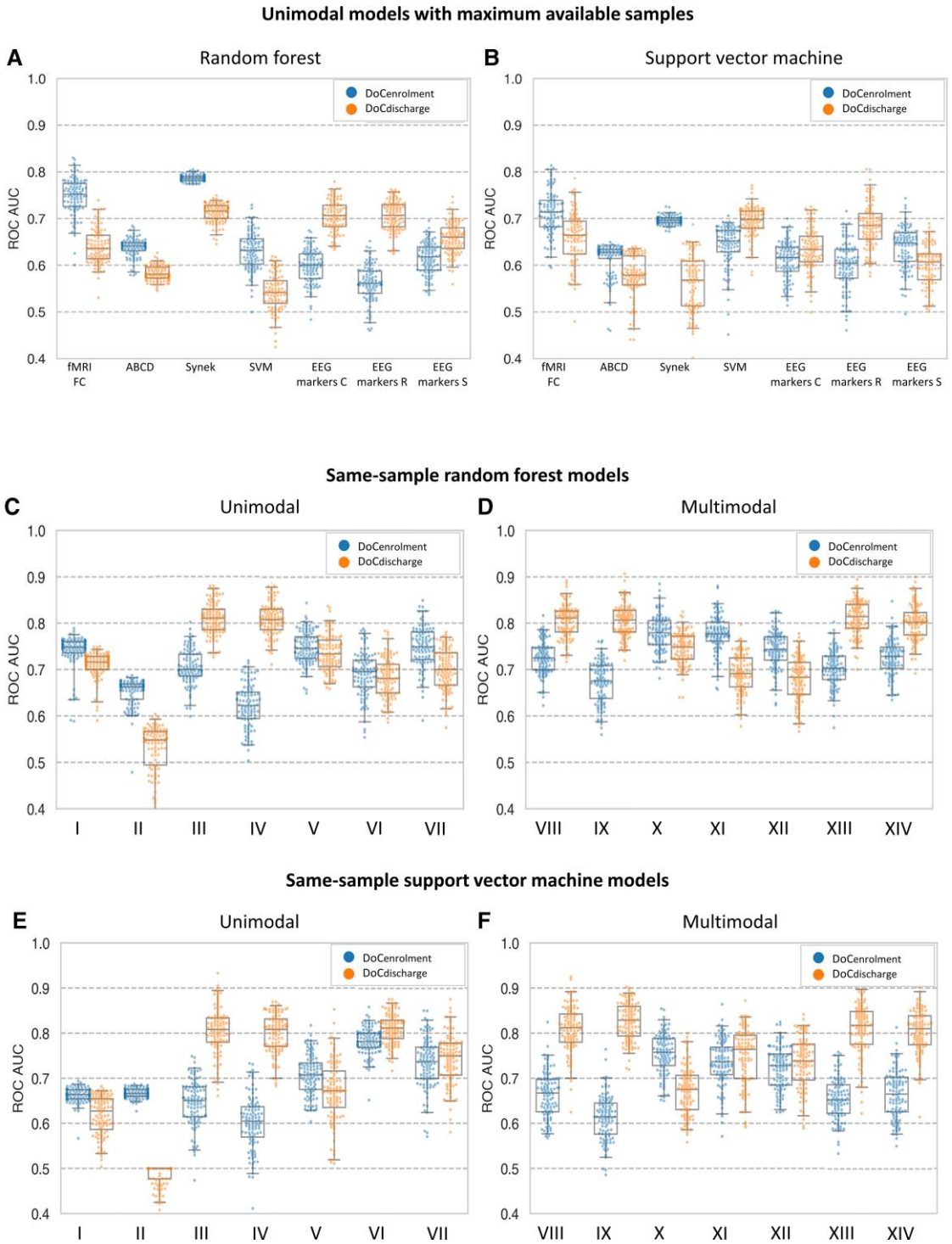

Figure 3 Unimodal models with maximum available data and same-sample models predicting levels of consciousness. Box plots illustrating model performances (AUCs) of Random Forest (**A**) and SVM (**B**) machine-learning models predicting $DoC_{enrolment}$ and $DoC_{discharge}$. Each model is based on the maximum amount of data available (see also Fig. 1, step 7). With the Random Forest models (**A**), the highest AUC for predicting $DoC_{enrolment}$ was obtained with the Synek categories (0.79; 95% CI 0.77–0.80), while the highest AUCs for predicting $DoC_{discharge}$ were obtained with Synek categories (0.71; 95% CI 0.66–0.74), EEG markers C (0.71; 95% CI 0.64–0.76) and EEG markers R (0.71; 95% CI 0.63–0.76). With the SVM models (**B**), the highest AUCs for predicting $DoC_{enrolment}$ were obtained with fMRI functional connectivity (FC) measures (0.71; 95% CI 0.62–0.81) and Synek categories (0.70; 95% CI 0.68–0.71), while the highest AUCs for predicting $DoC_{discharge}$ were obtained with the SVM classifier (0.69; 95% CI 0.62–0.75) and EEG markers R (0.68; 95% CI 0.60–0.78). (**C**–**F**) show Random Forest (**C** and **D**) and SVM (**E** and **F**) same-sample unimodal (**C** and **E**: models I–VII) and multimodal (**D** and **F**: models VIII–XIV) model performances (AUCs) when models are based on data from the exactly same patients ($n = 48$) with all available features [e.g. fMRI FC + Synek category + ABCD category + SVM classification of EEG segments (see also Fig. 1, steps 8 and 9)]. Of the unimodal same-sample models (**C**), all models except the ABCD model (model II) could predict level of consciousness at both enrolment and discharge above chance level. All multimodal models (**D**) could predict level of consciousness at both enrolment and discharge above chance level. In sum, this figure shows that all multimodal models (VIII–XIV) performed well with narrow CIs in predicting both $DoC_{enrolment}$ (AUCs ≥ 0.70 in six of seven models) and $DoC_{discharge}$ (AUCs ≥ 0.80 in five of seven models) (**D**), while the unimodal

(Continued)

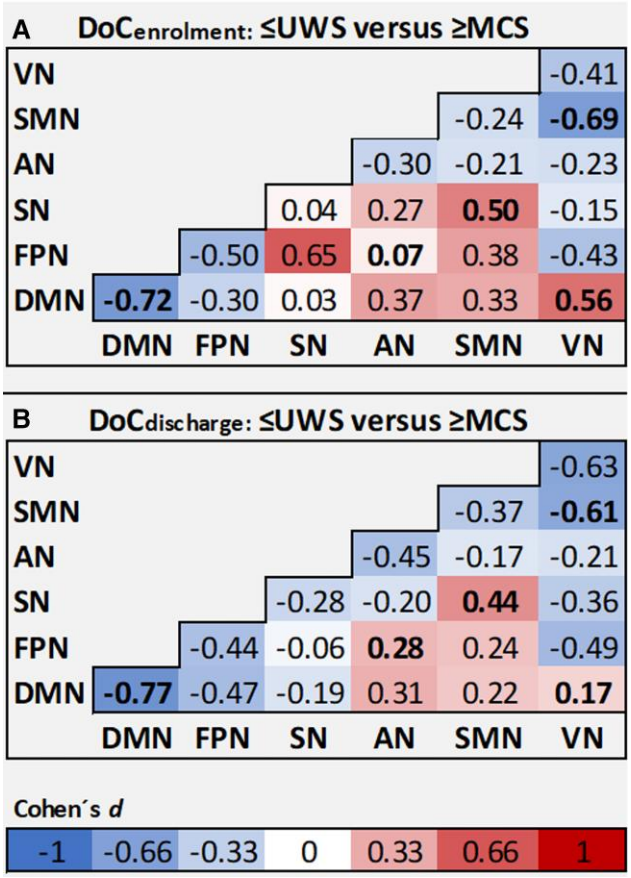

Figure 4 FMRI resting-state connectivity and association with levels of consciousness. Cohen's *d* effect size of resting-state network connectivity estimates in ≤UWS patients compared to ≥MCS patients at enrolment (**A**) and ICU discharge (**B**). At both study enrolment (**A**) and ICU discharge (**B**), a pattern of decreased DMN within-network connectivity and increased between-network connectivity is seen in ≤UWS patients compared to ≥MCS patients. Tiles are colour-coded according to increasing/decreasing effect size from 0. Bold values indicate statistical significance with unadjusted *P*-values (Enrolment: DMN–DMN: $P = 0.007$, DMN–VN: $P = 0.034$, FPN–AN $P = 0.009$, SN–SMN: $P = 0.047$, SMN–VN: $P = 0.006$; ICU discharge: DMN–DMN: $P = 0.001$, VN–VN: $P = 0.010$, FPN–VN: $P = 0.049$, SMN–VN: $P = 0.030$) when comparing ≤UWS to ≥MCS patients.

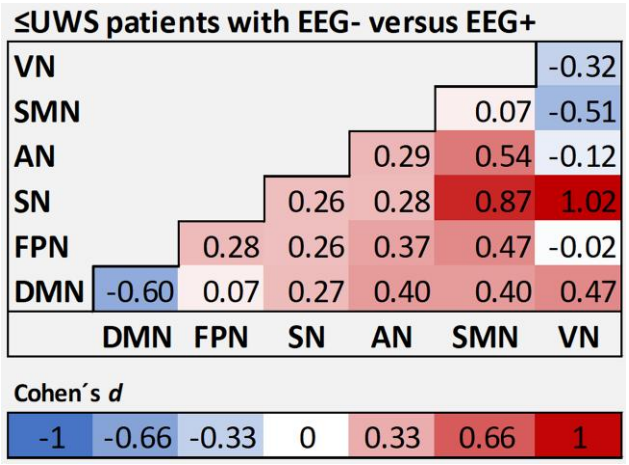

Figure 5 FMRI resting-state connectivity in ≤UWS patients with favourable EEG features. Cohen's *d* effect size of fMRI resting-state network connectivity estimates in patients classified as ≤UWS at enrolment with unfavourable EEG (EEG-) features compared to ≤UWS patients with favourable EEG (EEG+) features. In ≤UWS patients with unfavourable EEG features, the DMN within-network connectivity was decreased compared to ≤UWS patients with favourable EEG features. Tiles are colour-coded according to increasing/decreasing effect size from 0.

comparable to that of EEG models. While EEG models had high positive predictive value, fMRI models predicted consciousness levels at ICU discharge with better sensitivity. Thus, combining EEG and fMRI features to predict consciousness levels at ICU discharge resulted in high positive predictive value and sensitivity, which is important for clinical decision-making in the ICU.[6]

Patients with a disconnect between clinical exam and EEG/functional MRI

We identified a subgroup of patients ($n = 11$, 27.5%) clinically classified as ≤UWS but with favourable EEG features, suggesting higher levels of cortical activity than indicated by the clinical phenotype. As expected, this percentage is greater than the 15% of ICU patients with cognitive motor dissociation (CMD)[52] who could actively follow commands during EEG in a previous study.[9] Interestingly, the prevalence of 27.5% almost exactly matches the 25.6% of UWS patients in a meta-analysis on chronic DoC that showed evidence of residual consciousness, when assessed by passive fMRI or EEG paradigms.[7] It follows that residual consciousness in acute DoC patients seems at least as common as in chronic DoC patients.

Patients who are clinically ≤UWS but have favourable EEG or fMRI features may be genuinely unconscious (false positives), truly conscious (CMD) or have some degree of residual consciousness akin to 'covert cortical processing', also known as higher-order cortex motor dissociation' (HMD)[10,13] or 'cortically mediated states'.[53]

Although mental task-based active paradigms are highly specific at identifying CMD,[8] the sensitivity is low,[7,10] leading to many DoC patients with residual consciousness going undetected. Conversely, HMD patients can be identified without active paradigms. Passive and resting-state paradigms are therefore key to identifying HMD patients, especially because these paradigms are more straightforward to implement in the ICU.[7]

FMRI was available from 8 of 11 patients with favourable EEG features. Although not statistically significant, DMN within-network connectivity was numerically higher in patients with favourable EEG features compared to patients with unfavourable EEG features. Moreover, between-network connectivity in patients with unfavourable EEGs was increased (albeit not statistically significant). Thus, pathologically increased connectivity in these areas may be more pronounced in truly unconscious patients. Our results support previous findings of hyperconnectivity outside the DMN in chronic DoC patients.[50,51] Di Pierri *et al.*[51] assessed resting-state fMRI connectivity in chronic DoC patients and found decreased

Figure 3 Continued
models (**A–C**) in general performed with lower AUCs and wider CIs. A similar pattern was observed for SVM machine-learning models (**E** and **F**). Unimodal same-sample models: I = Synek, II = ABCD, III = EEG markers C, IV = EEG markers R, V = EEG markers S, VI = SVM and VII = fMRI FC. Multimodal same-sample models: VIII = fMRI FC + EEG markers C, IX = fMRI FC + EEG markers R, X = fMRI FC + markers S, XI = fMRI FC + Synek + ABCD + SVM, XII = Synek + ABCD + SVM, XIII = Synek + ABCD + SVM + EEG markers C and XIV = fMRI FC + Synek + ABCD + SVM + EEG markers C.

DMN connectivity and pathologically increased between-network connectivity with lower levels of consciousness, similar to our results in acute DoC patients.

In line with earlier reports,[5,54] the immediate cause of death in our ICU cohort was WLST (28/31; including $n = 27$ ≤UWS). This illustrates the importance of identifying patients with residual consciousness in ICU.[55–57] That said, the clinical trajectory of HMD patients is yet unknown and not necessarily equivalent to the trajectory of CMD patients, who are known to have better outcomes.[9,58–60]

Clinical benefit of combining EEG and functional MRI

Our primary aim was to evaluate the utility of combining EEG and fMRI measures for prognostication in the ICU. Although we believe our findings generally support this utility, there are nuanced interpretations to consider.

Our results do not clearly indicate an additive effect on performance of combining EEG and fMRI features. Generally, the combined models performed comparably to individual EEG and fMRI models. Notably, although the AUC for predicting consciousness level at ICU discharge from an SVM model using Synek categories was poorer than the SVM model based on EEG markers C (AUC = 0.62 versus 0.80, respectively), the sensitivity was 1 for $DoC_{discharge}$ using the Synek-based model, indicating that misclassification of ≥MCS patients as ≤UWS is not a problem. This is clinically relevant as this information can help avoid unjustified pessimistic decisions.[6]

The highest positive predictive value for $DoC_{discharge}$ was 0.82. This suggests that approximately one in five ≤UWS patients might be misclassified as ≥MCS, which appears acceptable, because, as pointed out, it is important in the ICU to predict consciousness recovery with high sensitivity to avoid premature WLST. Still, misclassifying truly unconscious patients as ≥MCS may result in prolonged futile treatment, which is burdensome for caregivers and puts a strain on limited healthcare resources. Thus, we suggest that an optimal prediction model should be based on a combination of fMRI functional connectivity and EEG features, resulting in a high overall performance, and optimal sensitivity and positive predictive value.

Altogether, our findings suggest that EEG and fMRI in a multimodal setup may be worthy of implementation in the clinic for better prognostication of acute DoC patients in the ICU, but this needs replication and validation in large, prospective multicentre studies including long-term follow-up.

Strengths and limitations

Designed to align with daily ICU management, CONNECT-ME is subject to limitations. Whereas previous studies have focused on patients with homogeneous conditions like TBI[13] or cardiac arrest,[35] our cohort was heterogeneous, reflecting the real-life variety of brain disorders in ICU.

The decision to enrol only patients with a clinical indication for structural MRI introduced bias in several contrasting ways. As MRI is logistically challenging in the ICU,[6] MRI may be used more frequently in a subset of patients with poor prognosis to review the full extent of brain damage prior to deciding about WLST.[6] Conversely, because MRI is easier to perform in more stable patients, a subset of patients with better prognosis may also undergo MRI more frequently than the average ICU patient.

The Coma Recovery Scale-Revised (CRS-R)[61] is the gold standard for classifying consciousness levels in chronic DoC,[3] but is rarely used for acute DoC in the ICU because it is time-consuming (a limitation also acknowledged by the recent European Academy of Neurology guideline on coma and DoC).[16,62] Although we did not use the CRS-R, our systematic neurological exam assessed its essential subelements (comparably to a novel abbreviated consciousness scale,[63] published 3 years after CONNECT-ME was initiated). We furthermore supplemented our exam with the FOUR scale, which is especially suitable for intubated patients.[27] Finally, we documented repeated observations from the daily routine exams performed by ICU staff to account for fluctuations in consciousness levels. All these measures reduced the risk of missing clinical signs of residual consciousness.

For practical reasons, we sampled levels of consciousness at the time of fMRI and again at ICU discharge. We acknowledge that this may have introduced some bias due to greater variability in the time periods compared to sampling consciousness levels at identical time intervals, e.g. every 14 days, starting from injury onset. However, we considered it more important to collect levels of consciousness at the time of fMRI and EEG to optimally evaluate the performance of the two measurements.

Levels of consciousness at ICU discharge in patients who died due to WLST were determined as soon as the decision to withdraw therapy was made. Theoretically, this might have influenced investigators evaluating these patients just before the start of palliative care. However, if present, we think the bias was minor because we always checked the results of the final examination against the clinical observations of the ICU staff just prior to the WLST decision.

Finally, one must keep in mind that initially, we enrolled patients on convenience sampling, which may affect the generalizability of our results to some extent.

The major strength of our study is the multimodal approach with repeated bedside examinations, EEG recordings and fMRI scans, including analysis by two different machine-learning algorithms, in a large cohort of acutely brain-injured ICU patients. This real-life setting makes CONNECT-ME generalizable to the management of ICU patients suffering from acute DoC due to various causes of brain injury.

To fully appreciate the extent of challenges, one must bear in mind the logistics of the ICU environment. FMRI, particularly, is difficult to obtain with various factors affecting data quality: (i) critically unstable patients often cannot be safely transported to the MRI, and they need monitoring during image acquisition, which puts strains on anesthesiology staff resources; (ii) not all patients can be fully weaned from sedation during fMRI; (iii) extra- and intracranial devices can cause MRI signal dropout or may contraindicate acquisition of fMRI; (iv) MR scanners of different magnetic strength were used according to contraindications and availability; (v) morphological brain abnormalities may undermine signal quality; (vi) we included patients irrespective of age, which may affect grey matter thickness and thus connectivity estimates; and (vii) there is heterogeneity in MRI acquisition parameters. EEG is safe and more easily available at bedside, but electrical noise in the ICU challenges the acquisition of high-quality EEG recordings.[64] Finally, keeping the delay between the neurological exam, EEG and fMRI to a minimum requires coordination between all involved staff, including neuroanaesthesiologists, neurologists, neurosurgeons, cardiologists, radiologists, nurses, radiographers, EEG technicians and the research team. At any given time, sudden deterioration of the patient can necessitate postponement or cancellation of investigations.

The above challenges may be the reason that, to our knowledge, investigating acute DoC by EEG and fMRI has not yet been accomplished in a similar-sized ICU cohort as ours.

Conclusions

In unresponsive patients with acute brain injury, EEG and fMRI measures classified consciousness levels during ICU admission both alone and in combination, with overall equal performance. Although machine-learning models based on EEG features obtained a high level of positive predictive value with few false negatives, sensitivity was low. However, by combining individual EEG and fMRI-based models, an optimal combination of overall model performance, positive predictive value and sensitivity could be obtained. Importantly, regardless of the machine-learning algorithm used, this multimodal approach also enabled prediction of consciousness levels at ICU discharge.

Acknowledgements

We thank the EEG technicians at the Department of Clinical Neurophysiology, the MRI technicians at the Department of Radiology and the nursing staff of the Departments of Neuroanaesthesiology, Cardiology, Neurology and Intensive Care, all at Rigshospitalet, Copenhagen University Hospital, for their cooperation and support. Last, but not least, we are grateful for the patients and families who participated in this study.

Funding

This work was funded by Offerfonden (https://civilstyrelsen.dk/sagsomraader/raadet-for-offerfonden). Material execution, content and results are the sole responsibility of the authors. The assessments and views expressed in the material are the authors' own and are not necessarily shared by the Offerfonden. Additional funding was supplied by Region Hovedstadens Forskningsfond (https://www.regionh.dk/til-fagfolk/Forskning-og-innovation/finansiering-og-fonde/s%C3%B8g-regionale-midler/Sider/Region-Hovedstadens-forskningsmidler.aspx), Lundbeck Foundation and Rigshospitalets Forskningspuljer (https://www.forskningspuljer-rh.dk/).

Competing interests

The authors report no competing interests.

Supplementary material

Supplementary material is available at *Brain* online.

References

1. Majdan M, Plancikova D, Brazinova A, *et al*. Epidemiology of traumatic brain injuries in Europe: A cross-sectional analysis. *Lancet Public Health*. 2016;1:e76-e83.
2. Rosenfeld JV, Maas AI, Bragge P, Morganti-Kossmann MC, Manley GT, Gruen RL. Early management of severe traumatic brain injury. *Lancet*. 2012;380:1088-1098.
3. Schnakers C, Vanhaudenhuyse A, Giacino J, *et al*. Diagnostic accuracy of the vegetative and minimally conscious state: Clinical consensus *versus* standardized neurobehavioral assessment. *BMC Neurol*. 2009;9:35.
4. Kondziella D, Frontera JA. Pearls & Oy-sters: eyes-open coma. *Neurology*. 2021;96:864-867.
5. Turgeon AF, Lauzier F, Simard JF, *et al*. Mortality associated with withdrawal of life-sustaining therapy for patients with severe traumatic brain injury: A Canadian multicentre cohort study. *CMAJ*. 2011;183:1581-1588.
6. Albrechtsen SS, Riis RGC, Amiri M, *et al*. Impact of MRI on decision-making in ICU patients with disorders of consciousness. *Behav Brain Res*. 2022;421:113729.
7. Kondziella D, Friberg CK, Frokjaer VG, Fabricius M, Møller K. Preserved consciousness in vegetative and minimal conscious states: Sstematic review and meta-analysis. *J Neurol Neurosurg Psychiatry*. 2016;87:485-492.
8. Owen AM, Coleman MR, Boly M, Davis MH, Laureys S, Pickard JD. Detecting awareness in the vegetative state. *Science*. 2006;313:1402.
9. Claassen J, Doyle K, Matory A, *et al*. Detection of brain activation in unresponsive patients with acute brain injury. *N Engl J Med*. 2019;380:2497-2505.
10. Edlow BL, Claassen J, Schiff ND, Greer DM. Recovery from disorders of consciousness: Mechanisms, prognosis and emerging therapies. *Nat Rev Neurol*. 2021;17:135-156.
11. Bruno MA, Vanhaudenhuyse A, Thibaut A, Moonen G, Laureys S. From unresponsive wakefulness to minimally conscious PLUS and functional locked-in syndromes: Recent advances in our understanding of disorders of consciousness. *J Neurol*. 2011;258:1373-1384.
12. Cole DM, Smith SM, Beckmann CF. Advances and pitfalls in the analysis and interpretation of resting-state FMRI data. *Front Syst Neurosci*. 2010;4:8.
13. Edlow BL, Chatelle C, Spencer CA, *et al*. Early detection of consciousness in patients with acute severe traumatic brain injury. *Brain*. 2017;140:2399-2414.
14. Bodien YG, Chatelle C, Edlow BL. Functional networks in disorders of consciousness. *Semin Neurol*. 2017;37:485-502.
15. Giacino JT, Katz DI, Schiff ND, *et al*. Practice guideline update recommendations summary: Disorders of consciousness. *Neurology*. 2018;91:450-460.
16. Kondziella D, Bender A, Diserens K, *et al*. European academy of neurology guideline on the diagnosis of coma and other disorders of consciousness. *Eur J Neurol*. 2020;27:741-756.
17. Golkowski D, Merz K, Mlynarcik C, *et al*. Simultaneous EEG-PET-fMRI measurements in disorders of consciousness: An exploratory study on diagnosis and prognosis. *J Neurol*. 2017;264:1986-1995.
18. Frohlich J, Crone JS, Johnson MA, *et al*. Neural oscillations track recovery of consciousness in acute traumatic brain injury patients. *Hum Brain Mapp*. 2022;43:1804-1820.
19. Skibsted AP, Amiri M, Fisher PM, *et al*. Consciousness in neurocritical care cohort study using fMRI and EEG (CONNECT-ME): Protocol for a longitudinal prospective study and a tertiary clinical care service. *Front Neurol*. 2018;9:1012.
20. Bruno MA, Laureys S, Demertzi A. Coma and disorders of consciousness. *Handb Clin Neurol*. 2013;118:205-213.
21. Giacino JT, Ashwal S, Childs N, *et al*. The minimally conscious state: Definition and diagnostic criteria. *Neurology*. 2002;58:349-353.
22. DASAIM. Sedationsstrategi - Målrettet behandling af gener forbundet med kritisk sygdom. *Guidel - Dansk Selsk Anæstesiologi og Intensiv Med*. 2020;3:1-39.
23. Harris PA, Taylor R, Minor BL, *et al*. The REDCap consortium: Building an international community of software platform partners. *J Biomed Inform*. 2019;95:103208.
24. Kondziella D, Fisher PM, Larsen VA, *et al*. Functional MRI for assessment of the default mode network in acute brain injury. *Neurocrit Care*. 2017;27:401-406.
25. Othman MH, Bhattacharya M, Møller K, *et al*. Resting-state NIRS–EEG in unresponsive patients with acute brain injury: A proof-of-concept study. *Neurocrit Care*. 2021;34:31-44.

26. Teasdale G, Jennett B. Assessment of coma and impaired consciousness. A practical scale. *Lancet*. 1974;304:81-84.
27. Wijdicks EFM, Bamlet WR, Maramattom BV, Manno EM, McClelland RL. Validation of a new coma scale: The FOUR score. *Ann Neurol*. 2005;58:585-593.
28. Acharya JN, Acharya VJ. Overview of EEG montages and principles of localization. *J Clin Neurophysiol*. 2019;36:325-329.
29. Hirsch LJ, Laroche SM, Gaspard N, *et al*. American Clinical neurophysiology society's standardized critical care EEG terminology: 2012 version. *J Clin Neurophysiol*. 2013;30:1-27.
30. Beniczky S, Aurlien H, Brøgger JC, *et al*. Standardized computer-based organized reporting of EEG: SCORE. *Epilepsia*. 2013;54:1112-1124.
31. André-Obadia N, Zyss J, Gavaret M, *et al*. Recommendations for the use of electroencephalography and evoked potentials in comatose patients. *Neurophysiol Clin*. 2018;48:143-169.
32. Leitinger M, Beniczky S, Rohracher A, *et al*. Salzburg consensus criteria for non-convulsive status epilepticus—Approach to clinical application. *Epilepsy Behav*. 2015;49:158-163.
33. Admiraal MM, van Rootselaar AF, Horn J. Electroencephalographic reactivity testing in unconscious patients: A systematic review of methods and definitions. *Eur J Neurol*. 2017;24:245-254.
34. Synek VM. Prognostically important EEG coma patterns in diffuse anoxic and traumatic encephalopathies in adults. *J Clin Neurophysiol*. 1988;5:161-174.
35. Forgacs PB, Frey HP, Velazquez A, *et al*. Dynamic regimes of neocortical activity linked to corticothalamic integrity correlate with outcomes in acute anoxic brain injury after cardiac arrest. *Ann Clin Transl Neurol*. 2017;4:119-129.
36. Schomer DL, Da Silva FL. *Niedermeyer's electroencephalography: basic principles, clinical applications, and related fields*. 7th ed. Lippincott Williams & Wilkins (LWW); 2019.
37. Thomson DJ. Spectrum estimation and harmonic analysis. *Proc IEEE*. 1982;70:1055-1096.
38. Engemann DA, Raimondo F, King JR, *et al*. Robust EEG-based cross-site and cross-protocol classification of states of consciousness. *Brain*. 2018;141:3179-3192.
39. Sitt JD, King JR, El Karoui I, *et al*. Large scale screening of neural signatures of consciousness in patients in a vegetative or minimally conscious state. *Brain*. 2014;137:2258-2270.
40. Bekinschtein TA, Dehaene S, Rohaut B, Tadel F, Cohen L, Naccache L. Neural signature of the conscious processing of auditory regularities. *Proc Natl Acad Sci USA*. 2009;106:1672-1677.
41. Platt JC, Platt JC. Probabilistic outputs for support vector machines and comparisons to regularized likelihood methods. Adv LARGE MARGIN Classif. 1999:61-74. http://citeseer.ist.psu.edu/viewdoc/summary?doi=10.1.1.41.1639. Accessed 17 April 2022.
42. Behzadi Y, Restom K, Liau J, Liu TT. A component based noise correction method (CompCor) for BOLD and perfusion based fMRI. *Neuroimage*. 2007;37:90-101.
43. Demertzi A, Tagliazucchi E, Dehaene S, *et al*. Human consciousness is supported by dynamic complex patterns of brain signal coordination. *Sci Adv*. 2019;5:eaat7603.
44. Breiman L. *Random forests*. Vol 45. Kluwer Academic Publishers; 2001.
45. Pedregosa F, Varoquaux G, Gramfort A, *et al*. Scikit-learn: Machine learning in Python. *J Mach Learn Res*. 2011;12:2825-2830.
46. Bagnato S, Boccagni C, Sant'Angelo A, Prestandrea C, Mazzilli R, Galardi G. EEG Predictors of outcome in patients with disorders of consciousness admitted for intensive rehabilitation. *Clin Neurophysiol*. 2015;126:959-966.
47. Vanhaudenhuyse A, Noirhomme Q, Tshibanda LJF, *et al*. Default network connectivity reflects the level of consciousness in non-communicative brain-damaged patients. *Brain*. 2010;133:161-171
48. Demertzi A, Antonopoulos G, Heine L, *et al*. Intrinsic functional connectivity differentiates minimally conscious from unresponsive patients. *Brain*. 2015;138(Pt 9):2619-2631.
49. Bodien YG, Threlkeld ZD, Edlow BL. Default mode network dynamics in covert consciousness. *Cortex*. 2019;119:571-574.
50. Wu X, Gao J-H, Weng X, *et al*. Intrinsic functional connectivity patterns predict consciousness level and recovery outcome in acquired brain injury. *J Neurosci*. 2015;35:12932-12946.
51. Di Perri C, Bahri MA, Amico E, *et al*. Neural correlates of consciousness in patients who have emerged from a minimally conscious state: A cross-sectional multimodal imaging study. *Lancet Neurol*. 2016;15:830-842.
52. Schiff ND. Cognitive motor dissociation following severe brain injuries. *JAMA Neurol*. 2015;72:1413-1415.
53. Naccache L. Minimally conscious state or cortically mediated state? *Brain*. 2018;141:949-960.
54. Izzy S, Compton R, Carandang R, Hall W, Muehlschlegel S. Self-fulfilling prophecies through withdrawal of care: Do they exist in traumatic brain injury, too? *Neurocrit Care*. 2013;19:347-363.
55. Span-Sluyter CAMFH, Lavrijsen JCM, Van Leeuwen E, Koopmans RTCM. Moral dilemmas and conflicts concerning patients in a vegetative state/unresponsive wakefulness syndrome: Shared or non-shared decision making? A qualitative study of the professional perspective in two moral case deliberations. *BMC Med Ethics*. 2018;19:10.
56. Foster C. It is never lawful or ethical to withdraw life-sustaining treatment from patients with prolonged disorders of consciousness. *J Med Ethics*. 2019;45:265-270.
57. Fins JJ, Bernat JL. Ethical, palliative, and policy considerations in disorders of consciousness. *Arch Phys Med Rehabil*. 2018;99:1927-1931.
58. Pan J, Xie Q, Qin P, *et al*. Prognosis for patients with cognitive motor dissociation identified by brain–computer interface. *Brain*. 2020;143:1177-1189.
59. Pistarini C, Maggioni G. Early rehabilitation of disorders of consciousness (DOC): Management, neuropsychological evaluation and treatment. *Neuropsychol Rehabil*. 2018;28:1319-1330.
60. Kowalski RG, Hammond FM, Weintraub AH, *et al*. Recovery of consciousness and functional outcome in moderate and severe traumatic brain injury. *JAMA Neurol*. 2021;78:548-557.
61. Giacino JT, Kalmar K, Whyte J. The JFK coma recovery scale-revised: Measurement characteristics and diagnostic utility. *Arch Phys Med Rehabil*. 2004;85:2020-2029.
62. Kondziella D, Menon D, Helbok R, *et al*. A precision medicine framework for classifying patients with disorders of consciousness: Advanced classification of consciousness endotypes (ACCESS). *Neurocrit Care*. 2021;35-(Suppl 1):27-36.
63. Sanz LRD, Aubinet C, Cassol H, *et al*. SECONDs administration guidelines: A fast tool to assess consciousness in brain-injured patients. *J Vis Exp*. 2021;2021:1-18.
64. Alvarez V, Rossetti AO. Clinical use of EEG in the ICU: Technical setting. *J Clin Neurophysiol*. 2015;32:481-485.